Electron-impact ionization of the Fe atom

M. S. Pindzola
Department of Physics, Auburn University, Auburn, Alabama 36849

D. C. Griffin
Department of Physics, Rollins College, Winter Park, Florida 32789

J. H. Macek
Department of Physics and Astronomy, University of Tennessee, Knoxville, Tennessee 37996
(Received 25 October 1994)

The electron-impact ionization of the Fe atom is calculated in a distorted-wave approximation. A prior form of the scattering amplitude, containing a mixture of atomic and ionic potentials, produces a giant resonance in the cross section. A post form of the scattering amplitude, containing only ionic potentials, produces a cross section devoid of shape resonances. Furthur calculations using both forms are made for various single-, double-, and triple-differential cross sections.

PACS number(s): 34.80.Dp

I. INTRODUCTION

The two outgoing electrons, following the electron-impact ionization of an N-electron atom, may be labeled the slow ejected electron and the fast scattered electron. For ionization from certain atoms and ions, the ejected electron wave function calculated in a V^{N-1} potential may exhibit a shape resonance due to term dependence in the continuum. A classic example is the ionization of the outer $3p^6$ subshell of Ar [1]. A large repulsive exchange term in the $3p^5kd\ {}^1P$ ejected wave reduces the overlap between the bound $3p$ orbital and the kd continuum orbital, causing a large reduction in both the photoionization and electron-ionization cross sections. Another well-studied example is the ionization of the $4d^{10}$ subshell along the Xe isonuclear [2] and isoelectronic [3] sequences. For ionization from certain atoms and ions, the scattered-electron wave function calculated in a V^N potential may also exhibit a shape resonance due to the multiple well structure of the effective potential. These giant resonances usually lead to a strong enhancement of the electron-ionization cross section [4–6].

The labeling of outgoing electrons following the electron-impact ionization of an N-electon atom, however, is only a convenience. The prior form of the scattering amplitude [7,8] requires the incident and scattered electrons to be calculated in a V^N potential, while the bound and ejected electrons are calculated in a V^{N-1} potential. A post form of the scattering amplitude [9,10] may also be formulated in which all electrons "see" a V^{N-1} potential. Although the two forms may give different predictions for the cross section at the level of lowest-order perturbation theory, they should yield identical results when higher-order terms are included [11]. In practice, however, the evaluation of specific higher-order terms is difficult, with the added complication that certain classes of terms must be summed to all orders to take into account long-range three-body Coulomb effects.

In this paper we present an example of electron ionization of an atom in which the post and prior forms of the lowest-order scattering amplitude give quite different predictions for the cross section. For the electron-impact ionization of Fe, the prior form of the scattering amplitude exhibits a giant resonance in the cross section, while the post form produces a smooth cross section devoid of any shape resonances. Instead of foraging into the world of higher-order perturbation theory, we thought experiment might help us decide which is the best lowest-order theory, at least for the electron ionization of Fe. Thus we present not only total ionization cross sections, but use both forms to predict various single-, double-, and triple-differential cross sections. As shown below, the total ionization cross section measurements on Fe by Freund *et al.* [12] certainly favor the post form of the scattering amplitude and the absence of giant resonances.

II. THEORY

The direct-ionization cross section for an atomic subshell may be calculated using a configuration-average distorted-wave method. The uncoupled quantum numbers involved are given by

$$e^-(k_i\ell_i) + A(n\ell)^w \rightarrow A(n\ell)^{w-1} + e^-(k_e\ell_e) + e^-(k_f\ell_f) \ , \tag{1}$$

where w is the occupation number of the atomic subshell $(n\ell)$ and the triads (k_i, k_e, k_f) and (ℓ_i, ℓ_e, ℓ_f) are the linear and angular momenta of the initial, ejected, and final scattering partial waves, respectively. The triple-differential cross section, in atomic units, is given by

$$\frac{d^3\sigma}{d\epsilon_e d\Omega_f d\Omega_e} = 16\pi^4 \frac{k_e k_f}{k_i} \frac{w}{2(4\ell+2)} \times \sum_{m_\ell, m_s} \sum_{m_{s_i}, m_{s_e}, m_{s_f}} |\langle \Phi_f^- | r_{12}^{-1} | \Phi_i^+ \rangle|^2 \ . \tag{2}$$

To derive the explicit form of the scattering amplitude $\langle\Phi_f^-|r_{12}^{-1}|\Phi_i^+\rangle$ of Eq. (2), we assume that the initial electron wave function is given by

$$\phi^+_{k_i m_{s_i}}(\mathbf{r}) = \frac{1}{(2\pi)^{\frac{3}{2}}}\frac{1}{k_i}\sum_{\ell_i}(2\ell_i+1)i^{\ell_i}e^{i(\sigma_{\ell_i}+\delta_{\ell_i})} \times\frac{R_{\epsilon_i\ell_i}(r)}{r}P_{\ell_i}(\cos\theta)\chi_{m_{s_i}}\ , \tag{3}$$

the ejected electron wave function is given by

$$\phi^-_{k_e m_{s_e}}(\mathbf{r}) = \frac{1}{(2\pi)^{\frac{3}{2}}}\frac{1}{k_e}\sum_{\ell_e}(2\ell_e+1)i^{\ell_e}e^{-i(\sigma_{\ell_e}+\delta_{\ell_e})} \times\frac{R_{\epsilon_e\ell_e}(r)}{r}P_{\ell_e}(\hat{k_e}\cdot\hat{r})\chi_{m_{s_e}}\ , \tag{4}$$

and the final electron wave function is given by

$$\phi^-_{k_f m_{s_f}}(\mathbf{r}) = \frac{1}{(2\pi)^{\frac{3}{2}}}\frac{1}{k_f}\sum_{\ell_f}(2\ell_f+1)i^{\ell_f}e^{-i(\sigma_{\ell_f}+\delta_{\ell_f})} \times\frac{R_{\epsilon_f\ell_f}(r)}{r}P_{\ell_f}(\hat{k_f}\cdot\hat{r})\chi_{m_{s_f}}\ . \tag{5}$$

In Eqs. (3)–(5), the reduced radial wave function $R_{\epsilon\ell}$ is normalized to one times a sine function, P_ℓ is a Legendre polynomial, σ_ℓ is the Coulomb phase shift, and δ_ℓ is the distorted-wave potential phase shift. The scattering amplitude is given by

$$\begin{aligned}\langle\Phi_f^-|r_{12}^{-1}|\Phi_i^+\rangle = {}& \frac{\sqrt{2}}{\pi^2 k_i k_e k_f}\sum_{\ell_i,\ell_e,\ell_f}(2\ell_i+1)\sqrt{(2\ell+1)(2\ell_e+1)(2\ell_f+1)}\\ &\times i^{\ell_i-\ell_e-\ell_f}e^{i(\sigma_{\ell_i}+\sigma_{\ell_e}+\sigma_{\ell_f}+\delta_{\ell_i}+\delta_{\ell_e}+\delta_{\ell_f})}\sum_{m_{\ell_e},m_{\ell_f}}(-1)^{m_{\ell_e}+m_{\ell_f}}Y_{\ell_e m_{\ell_e}}(\hat{k_e})Y_{\ell_f m_{\ell_f}}(\hat{k_f})\\ &\times\Bigg[\delta_{m_{s_e},m_s}\delta_{m_{s_f},m_{s_i}}\sum_{\lambda_d}\begin{pmatrix}\ell_e & \lambda_d & \ell\\ 0 & 0 & 0\end{pmatrix}\begin{pmatrix}\ell_f & \lambda_d & \ell_i\\ 0 & 0 & 0\end{pmatrix}\\ &\times\sum_{q_d}(-1)^{q_d}\begin{pmatrix}\ell_e & \lambda_d & \ell\\ -m_{\ell_e} & -q_d & m_\ell\end{pmatrix}\begin{pmatrix}\ell_f & \lambda_d & \ell_i\\ -m_{\ell_f} & q_d & 0\end{pmatrix}R_{\lambda_d}\\ &-\delta_{m_{s_e},m_{s_i}}\delta_{m_{s_f},m_s}\sum_{\lambda_x}\begin{pmatrix}\ell_f & \lambda_x & \ell\\ 0 & 0 & 0\end{pmatrix}\begin{pmatrix}\ell_e & \lambda_x & \ell_i\\ 0 & 0 & 0\end{pmatrix}\\ &\times\sum_{q_x}(-1)^{q_x}\begin{pmatrix}\ell_f & \lambda_x & \ell\\ -m_{\ell_f} & -q_x & m_\ell\end{pmatrix}\begin{pmatrix}\ell_e & \lambda_x & \ell_i\\ -m_{\ell_e} & q_x & 0\end{pmatrix}R_{\lambda_x}\Bigg]\ ,\end{aligned} \tag{6}$$

where R_λ is the usual Slater radial integral and $Y_{\ell m}$ is a spherical harmonic. For the special case considered in this paper of back-to-back coplanar scattering ($\hat{k_e} = -\hat{k_f}$), the scattering amplitude becomes

$$\begin{aligned}\langle\Phi_f^-|r_{12}^{-1}|\Phi_i^+\rangle = {}& \frac{\sqrt{2}}{\pi^2 k_i k_e k_f}\sum_{\ell_i,\ell_e,\ell_f,L}\sqrt{\frac{(2\ell+1)(2L+1)}{4\pi}}(2\ell_i+1)(2\ell_e+1)(2\ell_f+1)\\ &\times i^{\ell_i-\ell_e-\ell_f}e^{i(\sigma_{\ell_i}+\sigma_{\ell_e}+\sigma_{\ell_f}+\delta_{\ell_i}+\delta_{\ell_e}+\delta_{\ell_f})}(-1)^{m_\ell}\begin{pmatrix}\ell_e & \ell_f & L\\ 0 & 0 & 0\end{pmatrix}\begin{pmatrix}\ell & \ell_i & L\\ m_\ell & 0 & -m_\ell\end{pmatrix}Y_{Lm_\ell}(\hat{k_f})\\ &\times\Bigg[(-1)^{\ell_i}\delta_{m_{s_e},m_s}\delta_{m_{s_f},m_{s_i}}\sum_{\lambda_d}\begin{pmatrix}\ell_e & \lambda_d & \ell\\ 0 & 0 & 0\end{pmatrix}\begin{pmatrix}\ell_f & \lambda_d & \ell_i\\ 0 & 0 & 0\end{pmatrix}\begin{Bmatrix}\ell_e & \lambda_d & \ell\\ \ell_i & L & \ell_f\end{Bmatrix}R_{\lambda_d}\\ &-(-1)^{\ell}\delta_{m_{s_e},m_{s_i}}\delta_{m_{s_f},m_s}\sum_{\lambda_x}\begin{pmatrix}\ell_f & \lambda_x & \ell\\ 0 & 0 & 0\end{pmatrix}\begin{pmatrix}\ell_i & \lambda_x & \ell_e\\ 0 & 0 & 0\end{pmatrix}\begin{Bmatrix}\ell_f & \lambda_x & \ell\\ \ell_i & L & \ell_e\end{Bmatrix}R_{\lambda_x}\Bigg]\ .\end{aligned} \tag{7}$$

If we integrate the triple-differential cross section over both solid angles Ω_e and Ω_f, Eqs. (2) and (6) reduce to a very simple form. The single-differential cross section is given by

$$\frac{d\sigma}{d\epsilon_e} = \frac{32w}{k_i^3 k_e k_f}\sum_{\ell_i,\ell_e,\ell_f}(2\ell_i+1)(2\ell_e+1)(2\ell_f+1) \times\left[\sum_{\lambda_d}\Xi_{\text{dir}}+\sum_{\lambda_x}\Xi_{\text{exc}}-\sum_{\lambda_d,\lambda_x}(-1)^{\lambda_d+\lambda_x}\Xi_{\text{int}}\right]\ , \tag{8}$$

where

$$\begin{aligned}\Xi_{\text{dir}} &= \begin{pmatrix}\ell_e & \lambda_d & \ell\\ 0 & 0 & 0\end{pmatrix}^2\begin{pmatrix}\ell_f & \lambda_d & \ell_i\\ 0 & 0 & 0\end{pmatrix}^2\frac{R^2_{\lambda_d}}{(2\lambda_d+1)}\ ,\\ \Xi_{\text{exc}} &= \begin{pmatrix}\ell_f & \lambda_x & \ell\\ 0 & 0 & 0\end{pmatrix}^2\begin{pmatrix}\ell_e & \lambda_x & \ell_i\\ 0 & 0 & 0\end{pmatrix}^2\frac{R^2_{\lambda_x}}{(2\lambda_x+1)}\ ,\\ \Xi_{\text{int}} &= \begin{pmatrix}\ell_e & \lambda_d & \ell\\ 0 & 0 & 0\end{pmatrix}\begin{pmatrix}\ell_f & \lambda_d & \ell_i\\ 0 & 0 & 0\end{pmatrix}\begin{pmatrix}\ell_f & \lambda_x & \ell\\ 0 & 0 & 0\end{pmatrix}\\ &\quad\times\begin{pmatrix}\ell_e & \lambda_x & \ell_i\\ 0 & 0 & 0\end{pmatrix}\begin{Bmatrix}\ell & \lambda_d & \ell_e\\ \ell_i & \lambda_x & \ell_f\end{Bmatrix}R_{\lambda_d}R_{\lambda_x}\ .\end{aligned} \tag{9}$$

Finally, the total ionization cross section is given by

$$\sigma = \int_0^{\frac{E}{2}} \frac{d\sigma}{d\epsilon_e} d\epsilon_e \ , \tag{10}$$

where $E = \epsilon_e + \epsilon_f = \epsilon_i - I$ and I is the subshell ionization potential.

The bound-state orbitals needed to evaluate the Slater radial integrals found in Eqs. (6)–(9) are generated using the Hartree-Fock wave function code developed by Cowan [13]. The continuum radial orbitals, or distorted waves, are calculated using a Hartree potential for the direct interaction and a local semiclassical approximation for the exchange interaction [14].

III. RESULTS

The results of configuration-average distorted-wave calculations for the total ionization cross section of Fe are shown in Fig. 1. The ground-state configuration of Fe is $3d^6 4s^2$. The subshell ionization potentials are $I_{4s} =$ 6.79 eV and $I_{3d} =$ 12.16 eV. The prior-form scattering-amplitude results are given by the dashed curve, which exhibits a giant resonance in both subshell cross sections. The post-form scattering-amplitude results are given by the solid curve and are devoid of shape resonance features. The experiment of Freund *et al.* [12] clearly favors the post-form results.

Configuration-resolved distorted-wave results for Fe can be easily obtained from the configuration-average results using the branching factors given by Sampson [15]. The ground LS term of Fe is $3d^6(^5D)4s^2\ ^5D$. By $4s$ subshell ionization, the ground LS term of Fe populates both the $3d^6(^5D)4s\ ^6D$ ground term and the $3d^6(^5D)4s\ ^4D$ excited term of Fe^+. In the remainder of this paper, we will focus on the ground-to-ground transition, which has an ionization potential of I =7.90 eV [16] and a cross section that is $\frac{3}{5}$ of the configuration-average cross section.

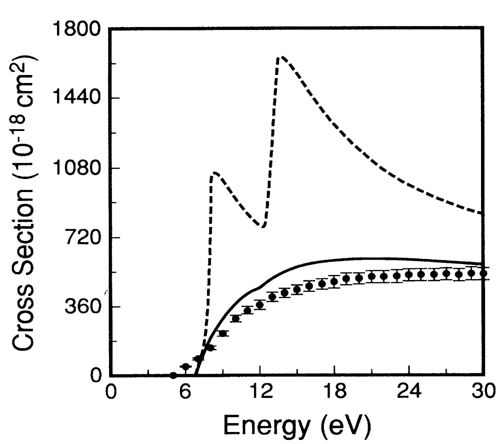

FIG. 1. Total ionization cross section for Fe. Dashed curve, prior form of the scattering amplitude, solid curve, post form of the scattering amplitude, solid circles, experimental measurements [12].

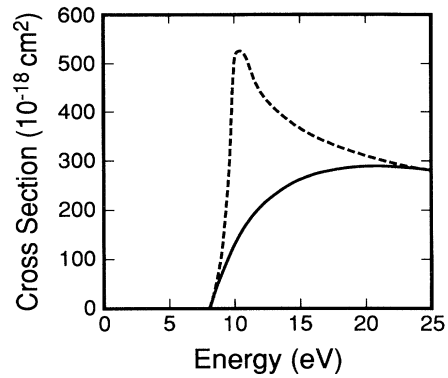

FIG. 2. $3p^6(^5D)4s^2\ ^5D \rightarrow 3d^6(^5D)4s\ ^6D$ total ionization cross section for Fe. Dashed curve, prior form of the scattering amplitude, solid curve, post form of the scattering amplitude.

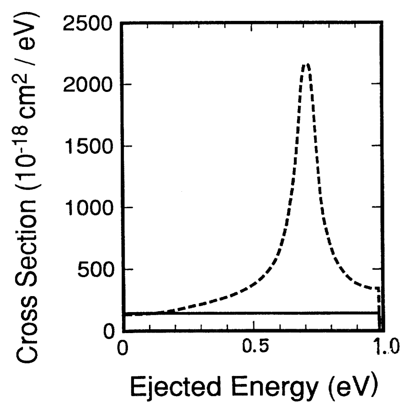

FIG. 3. $3p^6(^5D)4s^2\ ^5D \rightarrow 3d^6(^5D)4s\ ^6D$ single-differential ionization cross section for Fe at an incident energy of 9.88 eV. Dashed curve, prior form of the scattering amplitude; solid curve, post form of the scattering amplitude.

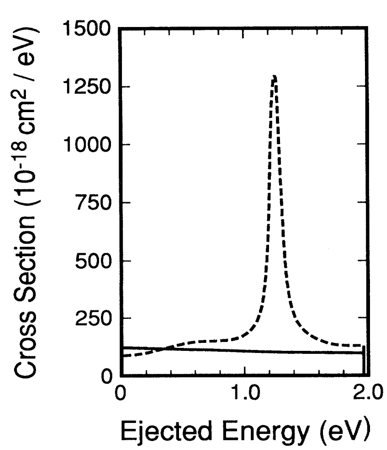

FIG. 4. $3p^6(^5D)4s^2\ ^5D \rightarrow 3d^6(^5D)4s\ ^6D$ single-differential ionization cross section for Fe at an incident energy of 11.85 eV. Dashed curve, prior form of the scattering amplitude; solid curve, post form of the scattering amplitude.

The post-form and prior-form results for this transition are shown in Fig. 2.

Single-differential cross section results for the $3d^6(^5D)4s^2\ ^5D \rightarrow 3d^6(^5D)4s\ ^6D$ transition in Fe are shown at two different incident electron energies in Figs. 3 and 4. For the prior form, the giant resonance occurs in the $\ell = 2$ final scattering channel at about $E_{\rm res} = 1.25$ eV. For $\epsilon_i = 9.88$ eV, as shown in Fig. 3, the resonance appears in the direct scattering amplitude and its peak in the differential cross section occurs at $\epsilon_e = \epsilon_i - I - E_{\rm res} = 0.73$ eV. For $\epsilon_i = 11.85$ eV, as shown in Fig. 4, the resonance appears in the exchange scattering amplitude and its peak in the differential cross section occurs at $\epsilon_e = E_{\rm res} = 1.25$ eV. For the post form, the single-differential cross section is almost flat.

Triple-differential cross-section results for the $3d^6(^5D)4s^2\ ^5D \rightarrow 3d^6(^5D)4s\ ^6D$ transition in Fe are shown at the same two incident-electron energies in Figs. 5 and 6. The scattering geometry is back-to-back coplanar. For $\epsilon_i = 9.88$ eV, as shown in Fig. 5, the ejected-electron energy is chosen to be at the peak of the giant resonance feature in the prior form, that is, $\epsilon_e = 0.73$ eV. Conservation of energy fixes the scattered electron energy at $\epsilon_f = \epsilon_i - I - \epsilon_e = 1.25$ eV, while geometry fixes the angles at $\theta_e = \theta_f + \pi$ and $\phi_e = \phi_f = 0$. The prior-form results shown in Fig. 5(a) are much larger and have a completely different angular dependence when compared to the post-form results shown in Fig. 5(b). For $\epsilon_i = 11.85$ eV, as shown in Fig. 6, $\epsilon_e = 1.25$ eV and $\epsilon_f = 2.70$ eV. The post-form and prior-form results for the triple-differential cross section are again completely different in shape and magnitude. An $(e,2e)$ experiment should have no trouble deciding between the two theoretical predictions.

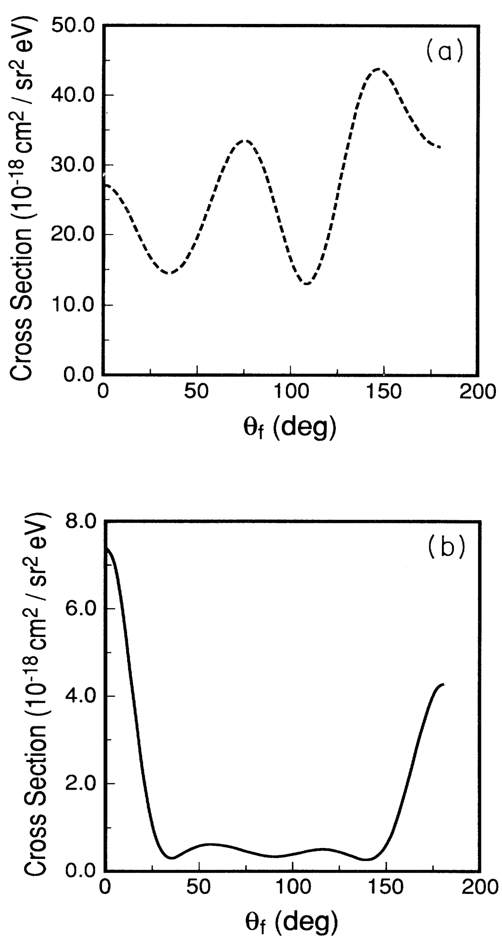

FIG. 5. $3p^6(^5D)4s^2\ ^5D \rightarrow 3d^6(^5D)4s\ ^6D$ triple-differential ionization cross section for Fe at an incident energy of 9.88 eV and an ejected energy of 0.73 eV. (a) Dashed curve, prior form of the scattering amplitude; (b) solid curve, post form of the scattering amplitude.

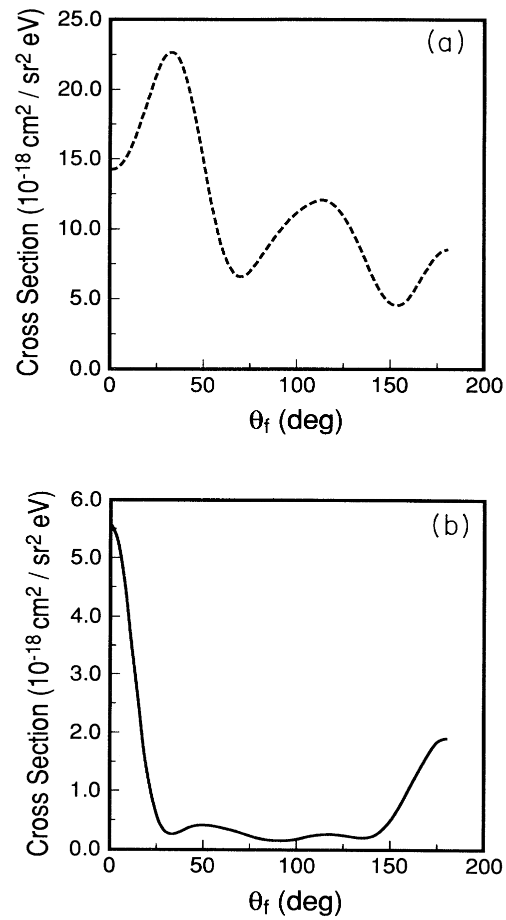

FIG. 6. $3p^6(^5D)4s^2\ ^5D \rightarrow 3d^6(^5D)4s\ ^6D$ triple-differential ionization cross section for Fe at an incident energy of 11.85 eV and an ejected energy of 1.25 eV. (a) Dashed curve, prior form of the scattering amplitude; (b) solid curve, post form of the scattering amplitude.

As a furthur guide, we integrate the triple-differential cross sections in Figs. 5 and 6 over θ_f. For $\epsilon_i = 9.88$ eV, this integrated (double-differential) cross section is 321×10^{-18} cm^2/sr eV in the prior form and only 8.36×10^{-18} cm^2/sr eV in the post form. For $\epsilon_i = 11.85$ eV, this integrated cross section is 139×10^{-18} cm^2/sr eV in the prior form and only 5.14×10^{-18} cm^2/sr eV in the post form.

IV. SUMMARY

Using a prior form of the scattering amplitude, the electron-impact ionization cross section of the Fe atom is found to contain a giant resonance. A post form of the scattering amplitude produces an ionization cross section devoid of shape resonances. Both forms have certain appeals as first-order theories. The use of a V^N potential for the incident electron and the fast scattered electron and a V^{N-1} potential for the slower ejected electron is physically motivated. However, for incident energies just above the ionization threshold of the atom, the distinction between fast scattered electron and slow ejected electron becomes blurred and using a V^{N-1} potential for both escaping electrons seems reasonable. The Freund *et al.* [12] experiment for the total ionization cross section of Fe certainly favors the post form of the scattering amplitude.

We certainly do not advocate one form of the lowest-order scattering amplitude over another in all cases. For the electron ionization of He the post form of the scattering amplitude produces an ionization cross section about 10% larger at peak than the prior form results, which are themselves about 15% higher than experiment. Recent calculations by Griffin *et al.* [17] for the electron ionization of Ar and Cl atoms favor the prior form of the scattering amplitude in the presence of V^{N-1} term-dependent shape resonances. For multiply charged atomic ions there is not much difference between the two forms; since the higher the asymptotic charge the less difference between the V^N and V^{N-1} potentials. In fact, the giant resonance in the prior form results for Fe can be made to disappear by choosing to calculate the distorted waves in only a Hartree potential, ignoring the effects of scattering exchange. What we hope this example of the ionization of Fe has shown, however, is the need to develop new methods for the calculation of electron ionization of complex atoms. This may take the form of the inclusion of higher-order perturbation theory terms or by direct nonperturbative solution.

ACKNOWLEDGMENTS

This work was supported in part by the Office of Fusion Energy of the U.S. Department of Energy under Grant No. DE-FG05-86-ER53217 with Auburn University and Grant No. DE-FG05-93ER54218 with Rollins College.

[1] S. M. Younger, Phys. Rev. A **26**, 3177 (1982).
[2] M. S. Pindzola, D. C. Griffin, and C. Bottcher, J. Phys. B **16**, L355 (1983).
[3] S. M. Younger, Phys. Rev. A **37**, 4125 (1988).
[4] S. M. Younger, Phys. Rev. Lett. **56**, 2618 (1986).
[5] S. M. Younger, Phys. Rev. A **35**, 2841 (1987).
[6] M. S. Pindzola and D. C. Griffin, Phys. Rev. A **46**, 2486 (1992).
[7] S. M. Younger, Phys. Rev. A **22**, 111 (1980).
[8] H. Jakubowicz and D. L. Moores, J. Phys. B **14**, 3733 (1981).
[9] J. Botero and J. H. Macek, J. Phys. B **24**, L405 (1991).
[10] J. H. Macek and J. Botero, Phys. Rev. A **45**, R8 (1992).
[11] C. Pan and H. P. Kelly, Phys. Rev. A **41**, 3624 (1990).
[12] R. S. Freund, R. C. Wetzel, R. J. Shul, and T. R. Hayes, Phys. Rev. A **41**, 3575 (1990).
[13] R. D. Cowan, *The Theory of Atomic Structure and Spectra* (University of California Press, Berkeley, 1981).
[14] M. E. Riley and D. G. Truhlar, J. Chem. Phys. **63**, 2182 (1975).
[15] D. H. Sampson, Phys. Rev. A **34**, 986 (1986).
[16] C. E. Moore, *Atomic Energy Levels,* Natl. Bur. Stand. (U.S.) Circ. No. 34 (U.S. GPO, Washington, DC, 1970).
[17] D. C. Griffin, M. S. Pindzola, T. W. Gorczyca, and N. R. Badnell, Phys. Rev. A (to be published).